JOURNAL
OF THE AMERICAN CHEMICAL SOCIETY

VOLUME 95, NUMBER 23 NOVEMBER 14, 1973

Molecular Motion in Lipid Bilayers. A Nuclear Magnetic Resonance Line Width Study[1]

C. H. A. Seiter[2] and Sunney I. Chan*

Contribution No. 4643 from the Arthur Amos Noyes Laboratory of Chemical Physics, California Institute of Technology, Pasadena, California 91109. *Received February 17, 1973*

Abstract: A model of the molecular motional state of unsonicated lipid bilayers is derived from proton magnetic resonance (pmr) line width considerations. The pmr line widths of both chain protons and the protons of methyl groups are calculated using a computer program based on Anderson's stochastic theory of resonance line widths. Spin–lattice relaxation phenomena observed for protons in lipid bilayers are also explained in terms of the same motional model. Finally, the effects of sample sonication on the pmr line widths are discussed in the light of stochastic relaxation results.

Amphiphilic molecules, *e.g.*, soaps, lecithins, or surfactants, generally, can form bilayer structures in water resembling those found in cell membranes.[3–8] Recently many biologically motivated studies of these lipid bilayers[9–20] have tried to determine the degree of molecular mobility in the interior and at the surface of the bilayer. Although proton magnetic resonance (pmr) would be a natural tool for such mobility studies, efforts thus far have been hampered by lack of an adequate treatment of the unique motional averaging effects which are found in nmr spectra when molecular motion is significantly restricted.

These restricted motion effects may be seen most clearly in experiments performed on samples in which bilayer sheets are oriented parallel to glass plates.[16,17] The line width of the pmr signal arising from the hydrocarbon chain protons in these bilayers depends strongly on the angular orientation of the sample in the external magnetic field. This demonstrates that the motion of these chains in the interior of the bilayer is seriously restricted. It also shows the pmr line width of the protons on these chains to be purely dipolar in origin. The details of this angular dependence suggest that chain proton pairs can execute rapid (faster than 10^{-5} sec) motions about the chain axis. There must, however, be other types of motion present as well, since the chain proton line width (3000–6000 Hz) in the spectra of unoriented bilayers is narrower than would be expected from this type of motion alone. In this connection, it should be noted that the tumbling correlation time of unsonicated bilayer sheets is too long to produce any motional narrowing at all.

Since internuclear vectors between protons on the lipid molecules thus cannot tumble freely over all directions in space (this is the exact meaning of "restricted" in this context), the usual line width expression appropriate to isotropic, liquid-like systems cannot be used here. Rather, a treatment of the pmr spectra exhibited by lipid bilayers must start with the rigid

(1) This work was supported by Grant GM 14523 from the National Institute of General Medical Sciences, U. S. Public Health Service.
(2) Fannie and John Hertz Foundation Fellow, 1970–1973.
(3) M. deBroglie and E. Friedel, *C. R. Acad. Sci.*, **176**, 738 (1923).
(4) V. Luzzati and F. Husson, *J. Cell Biol.*, 12, 207 (1962).
(5) H. Davson and J. F. Danielli, "The Permeability of Natural Membranes," Cambridge University Press, London, 1952.
(6) J. D. Robertson, *Progr. Biophys. Biophys. Chem.*, **10**, 343 (1960).
(7) J. M. Steim, M. E. Tourtellotte, J. C. Reinert, R. N. McElhaney, and R. L. Rader, *Proc. Nat. Acad. Sci. U.S.*, **63**, 104 (1969).
(8) M. H. F. Wilkins, A. E. Blaurock, and D. M. Engelman, *Nature (London), New Biol.*, **230**, 72 (1971).
(9) Y. K. Levine and M. H. F. Wilkins, *Nature (London), New Biol.*, **230**, 69 (1971).
(10) A. G. Lee, N. J. M. Birdsall, and J. C. Metcalfe, *Biochemistry*, 12, 1650 (1973).
(11) W. L. Hubbell and H. M. McConnell, *Proc. Nat. Acad. Sci. U. S.*, **63**, 16 (1969).
(12) W. L. Hubbell and H. M. McConnell, *Proc. Nat. Acad. Sci., U. S.*, 64, 20 (1969).
(13) S. I. Chan, G. W. Feigenson, and C. H. A. Seiter, *Nature (London)*, **231**, 110 (1971).
(14) J. Charvolin and P. Rigny, *J. Magn. Resonance*, 4, 40 (1971).
(15) J. Charvolin and P. Rigny, *Nature (London), New Biol.*, **237**, 127 (1972).
(16) G. J. T. Tiddy, *Nature (London)*, **230**, 136 (1971).
(17) J. J. De Vries and H. J. C. Berendsen, *Nature (London)*, 221, 1139 (1969).
(18) K. D. Lawson and T. J. Flautt, *Mol. Crystallogr.*, 1, 241 (1966).
(19) Z. Veksli, N. J. Salsbury, and D. Chapman, *Biochim. Biophys. Acta*, **183**, 434 (1969).
(20) E. G. Finer, A. G. Flook, and H. Hauser, *Biochim. Biophys. Acta*, **260**, 59 (1972).

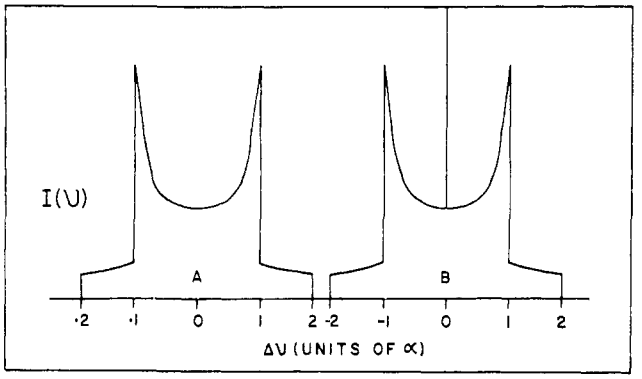

Figure 1. Dipolar powder spectra. (A) Nmr spectrum of isolated pairs of spins in a rigid lattice. (B) Nmr spectrum of isolated equilateral triangles of spins, when the triangles are allowed rapid reorientation about their threefold symmetry axis (the "methyl rotor" powder spectrum).

lattice powder spectra of these bilayers with the effects of various degrees of restricted local motion then introduced.

The only practical method for calculating such effects is the stochastic line width theory of Anderson,[21] or specifically the Monte Carlo version of this theory used by Saunders and Johnson.[22] Since this theory correctly describes all line width effects arising from motions whose correlation times are long compared with $1/\omega_0$ (ω_0 is the resonance frequency of the signal), this type of calculation can predict the results of any sort of motion, including isotropic as a special case.

Many amphiphilic molecules also contain, in addition to the methylene chain protons, both chain terminal methyl protons and methyl protons in the hydrophilic or polar region of the molecule. The pmr spectra of such molecules (*e.g.*, lecithins and alkyl trimethyl ammonium soaps) show relatively narrow methyl peaks, around 200 Hz in line width compared with 3000 Hz for methylene protons, which have significantly less intensity than would be expected from the methyl proton concentration in the sample.[23] These two observations can also be explained in terms of restricted motion effects. The Anderson theory can be used to introduce motional averaging into the powder spectrum of the three-spin group in this case.

Although Anderson's theory is well known to relaxation specialists, its application to the nmr of biological systems is novel and requires care in the definition of certain concepts. This paper therefore proceeds in three parts. The first part is a discussion of the Anderson theory and the terminology of motional narrowing as background for nonspecialists. Next, the application of this theory to pmr line widths observed in unsonicated lipid bilayers is discussed in detail, and the motional model which emerges from this treatment is examined in the light of spin–lattice relaxation results. Finally, the theory is modified to allow a treatment of the effects of sample sonication on lipid bilayer pmr line widths.

Method

Anderson showed that, for a resonance signal whose spin–spin relaxation rate T_2 is fast compared with its T_1, the free induction decay $g(t)$[24] associated with that resonance may be computed from the expression

$$g(t) = \overline{\exp\left(i\int_0^t \omega(\tau)\mathrm{d}\tau\right)} \qquad (1)$$

Here $\omega(\tau)$ is the resonance frequency of the transition and the bar denotes averaging over an ensemble of spins. In general, $\omega(\tau)$ is time dependent because of fluctuating local magnetic fields (dipolar, anisotropic chemical shift, etc.).

The above expression is best understood by considering a few familiar applications. The case of a spin experiencing only a static magnetic field $\mathbf{H}_0$ is the simplest. This gives $\omega(\tau) = \omega_0$ and hence $g(t) = \exp(i\omega_0 t)$. (In practice only $\cos \int_0^t \omega(\tau)\mathrm{d}\tau$ is usually computed, and the decay is made to refer to a frame rotating at frequency ω_0 so the absorption signal appears at zero frequency.) This elementary fixed-frequency case is easily extended to treat the static dipolar powder spectrum[25] for a sample of randomly oriented pairs of spins. Here the resonance frequency for a given orientation of a pair is given by

$$\omega = \pm\alpha(3\cos^2\theta - 1) \qquad (2)$$

where $\alpha = 3\mu^2/\hbar r^3$, and θ is the angle between $\mathbf{H}_0$ and the pair internuclear vector $\mathbf{r}$. μ denotes the magnetic moment for the spin. The dipolar powder spectrum which results from summing the set of frequencies over all possible pair orientations is shown in Figure 1A.

Another simple case, whose features suggest the fundamental issue in motional narrowing, treats a small local field H' jumping randomly between the values $+|H'|$ and $-|H'|$ at a rate $1/\tau_c$. If γ is the magnetogyric ratio for the spin species, then, in the rotating frame

$$\omega(\tau) = \gamma H'(\tau) \qquad (3)$$

and one can show from simple averaging arguments that

$$\int_0^t \omega(\tau)\mathrm{d}\tau \sim \gamma|H'|\sqrt{t\tau_c} \qquad (4)$$

for a typical series in $\omega(\tau)$. The decay $g(t)$ proceeds to $1/e$ of its initial value as this integral goes to 1 (indicating a mean dephasing of 1 radian). The time constant for this decay thus has the value

$$\frac{1}{T_2} \cong \gamma^2|H'|^2\tau_c \qquad (5)$$

The next level of application is to the problem of motional averaging of dipolar broadening, a case which has been treated both analytically (Fixman)[26] and numerically (Saunders and Johnson).[22] The dipolar field is still represented by eq 2, but $\theta(\tau)$ and hence $\omega(\tau)$ are now made time dependent by molecular reorientation, and the internuclear vector $\mathbf{r}$ described above is allowed to reorient randomly inside a sphere. The distribution of directions of $\mathbf{r}$ can be found by solving a diffusion equation or by actual dynamical simulation of the motion. The second procedure gives values of

(21) P. W. Anderson, *J. Phys. Soc. Jap.*, **9**, 316 (1954).
(22) M. Saunders and C. S. Johnson, Jr., *J. Chem. Phys.*, **48**, 534 (1968).
(23) C. H. A. Seiter, G. W. Feigenson, S. I. Chan, and M. C. Hsu, *J. Amer. Chem. Soc.*, **94**, 2535 (1972).
(24) R. Kubo and K. Tomita, *J. Phys. Soc. Jap.*, **9**, 888 (1954).
(25) G. E. Pake, *J. Chem. Phys.*, **16**, 327 (1948).
(26) M. Fixman, *J. Chem. Phys.*, **47**, 2808 (1967).

$\theta(\tau)$ and hence $\omega(\tau)$ directly after each step, and the integral $\int_0^t \omega(\tau)d\tau$ just becomes a sum. As would be expected, when the reorientation rate of **r** becomes fast compared with $1/\alpha$, the dipolar pattern collapses to a single Lorentzian line.

Extension to Restricted Motions

The extension of the procedure of Saunders and Johnson to the motional narrowing observed in pmr spectra of bilayers requires the introduction of constraints on the motion of the internuclear vectors. These constraints are designed to simulate a condition of *restricted* motion, a state which must be distinguished from the usual motional states in high resolution nmr. The most frequently encountered states there are simply *isotropic* and *anisotropic*. *Isotropic* describes motion which is unrestricted in space and can be characterized by a single motional correlation time τ_c. Anisotropic motion occurs when a body is still tumbling freely but has different rates of reorientation about different principal axes; *e.g.*, both $\tau_\perp$ and $\tau_\parallel$ are needed to specify the motions of a cigar-shaped body.

Restricted motion occurs when a body is no longer tumbling perfectly freely in space. This situation can have two origins. First, a cigar-shaped body could be confined, perhaps, in a loose-fitting cylinder, and its long axis could be free to cover only a small range of angles with respect to the cylinder direction. Second, a body could have a net statistical orientation, as in nematic liquid crystals or molecules oriented by applied electric fields. In both of these cases, the intramolecular dipolar fields will not be averaged to zero.

The average intramolecular dipolar field produced by each of these types of motion may be obtained either from a time average or a statistical average. The time average of these fluctuating fields

$$\overline{H'} \sim \langle 3\cos^2\theta(t) - 1\rangle_{av} \qquad (6)$$

can be replaced, for times long compared with 10^{-4} sec (the inverse of the dipolar line width in frequency units), by the statistical expression

$$\overline{H'} \sim \int_{\varphi_1}^{\varphi_2}\int_{\theta_1}^{\theta_2}(3\cos^2\theta - 1)P(\theta,\varphi)\sin\theta\, d\theta d\varphi \qquad (7)$$

Here $P(\theta,\varphi)$ is a statistical weighting function which accounts for the equilibrium distribution of directions that can be assumed by the direction of **r**, the internuclear vector.

For the case of isotropic motion, the domain of integration is the surface of the unit sphere (*i.e.*, $\theta \rightarrow [0,\pi]$, $\varphi \rightarrow [0,2\pi]$) and $P(\theta,\varphi)$ is constant, so $\overline{H'} = 0$. The distribution function P being constant means that all directions in space are equally likely for **r** after long times. Anisotropic motion as defined above satisfies the same conditions, differing from the isotropic case only in the rate at which $\overline{H'}$ approaches zero.

The case of restricted motion introduces the possibility of average fields $\overline{H'}$ not equal to zero. For example, a net statistical orientation of a molecule by an external electric field will produce a $P(\theta,\varphi)$ which is not constant and will reflect the preferred directions for **r**. This will give rise, in general, to average fields $\overline{H'}$ that are nonzero. The restricted motions which are considered in this paper specify distribution functions

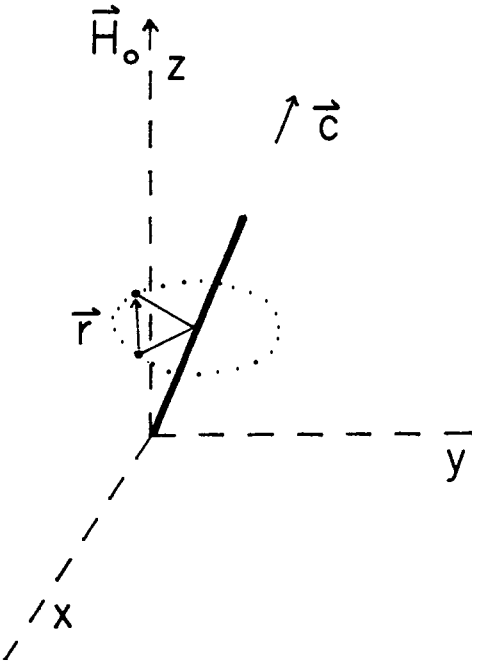

Figure 2. Definition of relevant angles. $\mathbf{H}_0$ is the direction of the applied magnetic field, **r** is the interproton vector, and **c** is the chain axis direction. The angle between r and $\mathbf{H}_0$ is called θ, the angle between **c** and $\mathbf{H}_0$ is called θ', and the angle between r and **c** is called β. The azimuthal angle φ is the difference between φ_c, the phase angle of the projection of **c** in the x–y plane, measured from y, and φ_r, the phase angle of **r** about **c**, again measured from y.

$P(\theta,\varphi)$ which are essentially rectangular and restrict the possible orientation directions of **r** to certain patches on the surface of the unit sphere. Since P is zero outside these allowed regions, the average $\overline{H'}$ could be found by restricting the domain of integration.

The angles which are used in this paper to characterize the restricted motion of protons on the lipid chains are described with reference to Figure 2. The angle θ between the internuclear vector **r** and the applied magnetic field $\mathbf{H}_0$ is the angle of physical interest, and it is calculated most conveniently in terms of β (the angle between **r** and the chain direction **c**), θ' (the angle between **c** and $\mathbf{H}_0$), and φ (the phase angle of **r** about **c** minus the phase angle of **c** about $\mathbf{H}_0$). The models of proton motion which will be investigated can be described by the amount of fluctuation they allow in β and φ. The value of $(3\cos^2\theta - 1)$ is evaluated in terms of β, θ', and φ by the addition theorem for spherical harmonics (see eq 32 below).

In the type of motion called case A, β is allowed to fluctuate over the range $[\bar{\beta} + \Delta\beta, \bar{\beta} - \Delta\beta]$ and φ can fluctuate freely. This model accounts for realistic proton motions, such as trans–gauche bond rotations or kink formation. Another type of motion, called case B, has the same restriction on β but an additional restriction of φ to a range $[\bar{\varphi} + \Delta\beta, \bar{\varphi} - \Delta\beta]$. This case represents restriction of the motion of pairs around the chain axis **c**, a condition which would occur in lipid dispersions below the crystalline $\rightleftharpoons$ liquid crystalline phase transition temperature.

Application

The computer program used here is a simple extension of that of Saunders and Johnson. Instead of allowing

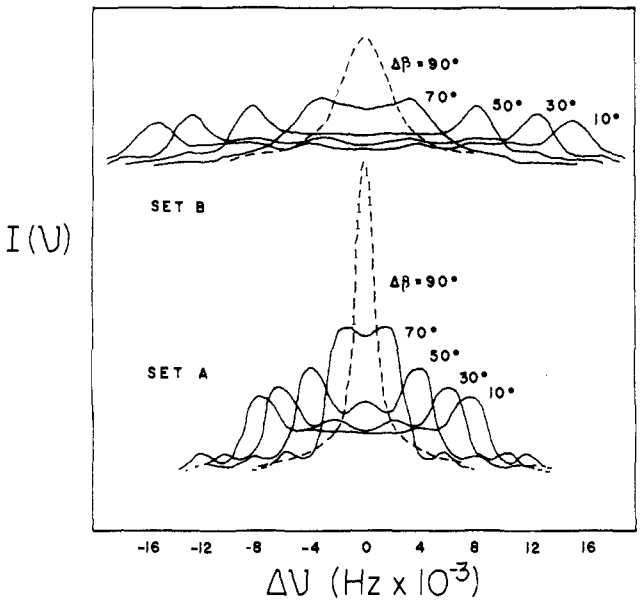

Figure 3. Dipolar powder spectra from isolated pairs of spins undergoing varying degrees of restricted motions of amplitude $\Delta\beta$, for two types of motion. Case A allows the spins reorientation about a **c** axis (Figure 2) and case B does not.

the direction of **r** to move over all directions, angular restrictions are imposed on the motion, resulting in the "random walk with reflecting barriers" described above. This random walk is generated by the computer program, and $g(t)$ is obtained from the frequency sequences generated by the random walk motion. All motional time scales in the program are defined in terms of $1/\alpha$. For motions like those shown in case A, it is possible to define two diffusion rates, one in $\Delta\beta$ and one for reorientation in the angle φ. Finally, the $g(t)$ obtained is transformed to frequency space using a fast Fourier transform algorithm.

In this section, results are first obtained for pairs of proton spins on chains undergoing restricted flexing motions. Next, the effects on this pair spectrum of other intramolecular methylene protons will be considered. Finally, spectra will be calculated for methyl group protons. The extension of this program to the calculation of spectra more complex than the two-spin dipolar case is straightforward. The powder spectrum of a methyl group, for example, has several sets of transitions,[27] and these transitions do not all have the same dependence on the orientation angles of the methyl group in the applied magnetic field. If the motion of the group does not make possible new types of transitions, but only perturbs the frequencies of those in the original spectrum, then the parts of the motionally averaged spectrum can be computed independently, following the frequency sequences generated by the motion of the group just as above. The application of this procedure to the methyl pmr spectrum is discussed below in detail.

Pairs of Spins. Calculated pmr spectra arising from isolated pairs of spins on chains undergoing various degrees of restricted motion are summarized in Figure 3. Two sets of simulated spectra are displayed, corresponding to the two types of motional restriction depicted in Figure 1 (set A corresponds to the motion in case A, set B to case B). Lorentzian background broadening has been superimposed on the spectra, 500 Hz in set A and 1000 Hz in set B. The background broadening was deliberately made small so that the two humps characteristic for the dipolar powder spectrum may still be seen. A more realistic broadening, accounting for neighbor protons outside the pair, would be comparable in magnitude to $\Delta\nu_{\text{eff}}$, the hump-to-hump splitting. The spectrum would then consist of a simple hump of width $\sim\Delta\nu_{\text{eff}}$ at half-height.

The motional correlation times used in the calculations were $\tau_\perp = {}^1/_5\alpha$ (sec) for motion in $\Delta\beta$ and $\tau_\parallel = {}^1/_{10}\alpha$ for reorientation about **c**. Values of $\tau_\perp$ faster than this produced no significant further averaging. In cases of restricted motion, the overall spectral width will depend only on the degree of restriction, as long as $\tau_\perp$ and $\tau_\parallel$ are sufficiently fast. The actual values of these correlation times must be determined from additional experiments, *e.g.*, magic angle orientation, Waugh multipulse dipolar narrowing studies, and T_1 measurements. Very slow correlation times ($\tau_\perp \geq 1/\alpha$) give no narrowing at all. This is a simple consequence of the fundamental principle in motion narrowing; *i.e.*, that to be effective in narrowing, a motion must cause fluctuations in the local fields which are fast compared with the inverse of the width of the frequency distribution these fields produce in the static case.

The motion of pairs about the **c** axis can be shown to reduce the effective width of the spectrum by one-half.[28] When the motion in φ is simulated directly, the spectra which result are essentially the same as those generated by replacing α by $\alpha/2$. Spectra obtained with this scaling factor are shown in Figure 3A. Since the exact shape of the free induction decay is more sensitive to the averaging method than these frequency spectra are, only free induction decays calculated by direct simulation are used for direct comparison with experiment (see below). The basis of the scaling effect used in Figure 3A is the average relationship

$$\overline{3\cos^2\theta - 1} = (3\cos^2\theta' - 1)\cdot\frac{1}{2}\overline{(3\cos^2\beta - 1)} \quad (8)$$

which is true for rapid motions in φ (see eq 32). When the appropriate ensemble average over values of θ' is taken, the two "bumps" of the powder pattern are expected to shift in toward the origin by $\sim$50% as compared with the case with restricted motion in φ.

The implications of this simple model are made clear by a comparison of calculated and experimental free induction decays. The experimental effective T_2 for all the protons in a sample of egg lecithin bilayers,[13] for example, is $\sim$120 μsec. This effective T_2 is the time at which the free induction decay has diminished to $1/e$ of its original value. What this relaxation time corresponds to in terms of local motions may be estimated from Table I. This table lists the effective T_2's calculated for proton pairs undergoing various degrees of restricted motion, of both the types considered in this paper. As can be seen at once, the case in which proton pairs can reorient about their **c** (chain) axis and execute fairly large ($\Delta\beta \sim 60°$) flexing motions most closely approximates the case of protons on lipid chains in bilayers. Since the greatest broadening influence

(27) H. M. McIntyre, T. B. Cobb, and C. S. Johnson, Jr., *Chem. Phys. Lett.*, 4, 585 (1970).

(28) H. S. Gutowsky and G. E. Pake, *J. Chem. Phys.*, 18, 162 (1950).

Table I. Effective T_2's for Proton Pairs Undergoing Various Degrees of Restricted Motion[a]

Case A		Case B	
$\Delta\beta$, deg	$T_{2(eff)}$, μsec	$\Delta\beta$, deg	$T_{2(eff)}$, μsec
10	32	10	14
30	38	30	18
50	70	50	25
60	100	60	45
70	180	70	72
90	260		

[a] Case A and case B refer to the motional situations described in the text.

on a given chain proton is the influence of its pair neighbor attached to the same carbon, the simple model of moving pairs gives a reasonably accurate representation of the motional narrowing situation for protons on lipid chains in bilayers.

The experimental free induction decay from protons in bilayers is compared with several calculated free induction decays for proton pairs undergoing restricted motions in Figure 4. Here the solid line is the first part of a reported[13] free induction decay from the protons in egg lecithin bilayers, and the dashed lines are calculated free induction decays for different amplitudes $\Delta\beta$ of restricted motion of type A (which includes motion about the chain axis). The first part of the experimental decay is taken because it represents mostly the free induction decay arising from the fast-relaxing methylene protons of the hydrocarbon chains in the bilayers, while the later parts of the free induction decay originate from the sharper methyl resonances. This plot shows that the free induction decay of these methylene protons strongly resembles that arising from pairs of spins undergoing restricted motions of amplitude $\Delta\beta \sim 60°$ while reorientating about a **c** axis.

Methylene Chain Protons. The results from the simple two-spin patterns suggested a calculation for chain protons that allowed reorientation about **c** the chain axis and motion in $\Delta\beta$ of amplitude $\sim 60°$. An attempt, however, must be made to include the effects of other protons on the chain as a more realistic model than the simple pair of spins. These other protons of the chain contribute a field at proton 1 of the pair which may be expressed in frequency units as

$$\omega' = \frac{3}{4}\gamma^2\hbar\sum_j (3\cos^2\theta_{1j} - 1)/r_{1j}^3 \qquad (9)$$

where the symbols have their usual interpretation. This expression is just the sum of the dipolar fields from individual protons. Since these fields are small[29] compared with that which produces the pair splitting, accounting for ω' in this way is as valid as solving for the splittings of the coupled n-spin system in terms of the angles θ_{1j}. If the protons reorient about the **c** axis, eq 9 may be rewritten as

$$\omega' = \frac{3}{8}\gamma^2\hbar(1 - 3\cos^2\theta')\sum_j [(3\cos^2\gamma_{1j} - 1)/r_{1j}^3] \qquad (10)$$

where θ' is the angle between **c** and $\mathbf{H}_0$ and γ_{1j} is the angle between **c** and a vector joining protons 1 and j.

This transformation is just a special case of the addition theorem for spherical harmonics and is analogous

(29) E. R. Andrew, *J. Chem. Phys.*, 18, 607 (1950).

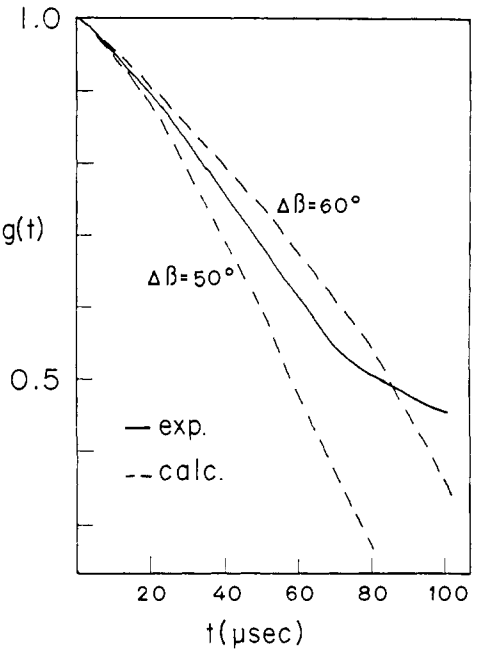

Figure 4. Calculated and experimental free induction decays. The experimental curve is the first part of the free induction decay from egg lecithin bilayers (see ref 13 of text). The calculated free induction decays arise from pairs of spins undergoing different amplitudes of restricted motion but unhindered reorientation about a **c** axis (Figure 2).

to the substitution (eq 8) performed earlier for reorientation about **c**. The relation

$$\omega_T = \frac{1}{2}(1 - 3\cos^2\theta')\left[\alpha(3\cos^2\beta - 1) + \alpha'\sum_j (3\cos^2\gamma_{1j} - 1)/r_{1j}^3\right] \qquad (11)$$

thus is sufficient for finding the $g(t)$ for a typical chain proton, including the broadening effects of chain neighbor protons. Appropriate restricted random walks are generated in β and the γ_{1j}'s, and a background broadening, small in terms of α, can be added as an intermolecular contribution.

Results of such a calculation, which allowed $\Delta\beta = 60°$, an effective $\Delta\gamma = 30°$, and 100-Hz Lorentzian intermolecular background broadening as an upper limit to the intermolecular contribution, are shown in Figure 5. The sharp line in the center refers to a sample in which **c** axes are oriented at 54° to $\mathbf{H}_0$, close to the magic angle. More pronounced magic angle effects are possible with orientation at 54°44′ but the very long $g(t)$ which results is rather expensive to compute. The principal effect of including these other chain protons in the calculation can be seen as a smoothing of the original features of the two-spin spectrum and an additional slight broadening ($\sim$10% increase in line width). Thus the two-spin dipolar spectra are a good approximation to the spectra of chain protons in bilayers.

An estimate of the intermolecular broadening contribution[10] used above for unsonicated bilayers can be obtained from the treatment of Kruger.[30] This investigator has given a procedure for estimating the contribution of intermolecular dipole–dipole inter-

(30) G. J. Kruger, *Z. Naturforsch. A*, 24, 560 (1969).

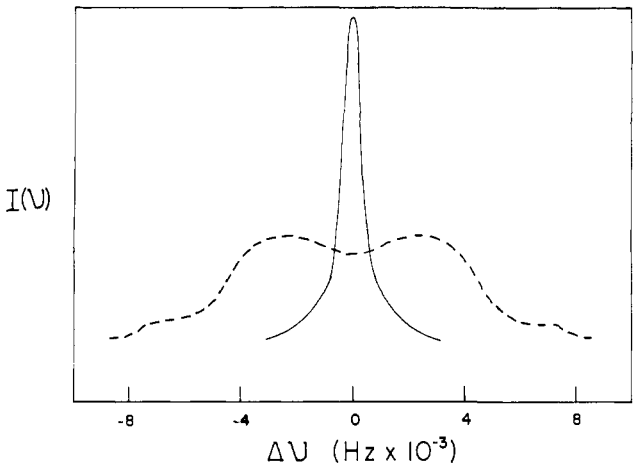

Figure 5. Motionally averaged dipolar spectra of methylene chain protons, including effects of intrachain neighbors. These protons are assumed to undergo restricted motion of type A with amplitude $\Delta\beta = 60°$. The dashed line is the spectrum arising from a randomly oriented collection of such chains, while the solid line is the spectrum arising from a collection of chains whose **c** axes are oriented at the "magic angle," $\theta' = 54°55'$ to the applied field $\mathbf{H}_0$.

actions to the line width and spin–lattice relaxation if this interaction is modulated by translational diffusion. In this particular case, lateral diffusion of lipid molecules causes the intermolecular dipolar fields at a given proton to fluctuate as the lipid chains exchange positions. Since chain protons may have $S_z = \pm 1/2$ with essentially equal probability, this position exchange among chains causes a proton to experience intermolecular fields fluctuating at a rate τ_{ex}, the chain position interchange time, which can be related to the lateral diffusion constant D. In phospholipid bilayers, D has been determined experimentally[31] and found to be 2×10^{-8} cm²/sec. This diffusion rate, when used in the theory of Kruger, gives a line width estimate of ~20 Hz, essentially independent of the detailed diffusion model. This prediction also agrees with the oriented-bilayer experiment of De Vries,[17] which demands that intermolecular broadening be less than ~100 Hz.

Methyl Protons. The powder spectrum of isolated rotating triangles of spins given by Andrew and Bersohn[32] is the starting point for calculations[33] of the restricted motional spectra of methyl protons. The spin Hamiltonian for an equilateral triangle of spins may be written as

$$\mathcal{H}' = -\gamma\hbar H_0 \sum_{i=1}^{3} I_{z_i} + \sum_{i>j}^{i=3} (\mathbf{I}_i \cdot \mathbf{I}_j - 3I_{z_i}I_{z_j})A_{ij} \quad (12)$$

where

$$A_{ij} = \frac{\gamma^2\hbar^2}{2r^3}(3\cos^2\theta_{ij} - 1) \quad (13)$$

The substitution $\cos\theta_{ij} = \cos\theta_m' \cos\beta_m + \sin\theta_m' \sin\beta_m \cos\varphi_{ij}$ can be used in eq 13 to show that rapid rotation of the three-spin group about its C_3 symmetry axis averages all the A_{ij}'s to the same value. Here θ_m' is the angle between the C_3 axis and the applied magnetic field $\mathbf{H}_0$, and $\beta_m = 90°$ is the angle between the $\mathbf{r}_{ij}$ and the C_3 axis. The average Hamiltonian then gives rise to a set of transitions at frequencies $-4x'$, 0, and $+4x'$, with intensity ratios of 1:2:1. Here x' has the value

$$x' = 1/4(\bar{A}_{12} + \bar{A}_{23} + \bar{A}_{13}) \quad (14a)$$

$$= \frac{3}{16}\frac{\gamma^2\hbar^2}{r^3}(1 - 3\cos^2\theta_m') \quad (14b)$$

The powder spectrum resulting from this set of transitions is shown in Figure 1B. This spectrum, characteristic of isolated rotating triangles of spins, has two main features: broad dipolar wings containing 50% of the spectral intensity, and a sharp central spike containing the rest of the intensity.

If these isolated rotating triangles are now allowed to undergo restricted motions of their C_3 axes, the dipolar wings of the spectrum will be motionally narrowed in the same way as a two-spin spectrum under the analogous restricted motion, but the central spike, whose frequency is angle independent, will still have zero width. Thus the width of this central methyl resonance (~200 Hz, as observed in delayed Fourier transform (FT) experiments on lecithin bilayers[23]) arises because the spins of the methyl triangles are not isolated but have neighboring spins, *e.g.*, methylene protons or other methyl groups. The line width of the methyl center spike, which is the resonance observed in delayed FT experiments (the dipolar wings being too broad), must be analyzed in terms of these "outside" dipolar fields, or specifically the average of these fields that the methyl protons experience as their C_3 axis undergoes restricted motions.

The outside dipolar fields are usually small compared with the splitting ($|4x'|$) produced by the spins in the methyl group. Furthermore, the closest protons to the triangle (*e.g.*, chain-CH_2 protons next to terminal methyls or methyl neighbors on a choline group) are rigidly connected to the C_3 axis of the methyl (a C–C or C–N bond). These outside fields can thus be described in terms of their angular dependence on θ_m', and the methyl spectrum can be calculated in exactly the same way as the chain proton spectrum of the previous section.

This procedure must be justified by showing that the center line, the main feature of interest in the methyl spectrum (ordinarily the broad wings will be lost in the methylene signal), behaves under the perturbation of the outside spin as if it arose from the single transition of a one-spin system. The average Hamiltonian appropriate to this problem is

$$\overline{\mathcal{H}''} = \overline{\mathcal{H}'} - \gamma\hbar H_0 I_{z_{ex}} + \sum_{i=1}^{3} (\mathbf{I}_{ex} \cdot \mathbf{I}_i - 3I_{z_{ex}}I_{z_i})\overline{A_{ex(i)}} \quad (15)$$

where the subscript ex denotes the outside spin, and the bar denotes averaging with respect to the three moving spins in the methyl group. When applied to the spin functions listed in Table II for the four-spin problem, this Hamiltonian produces in the center of the spectrum a pair of lines at $\pm 4/3x''$ and satellites of negligible intensity at $\pm 4x''$ and $\pm 2/3x''$, where $x'' = 1/4\Sigma_{i=1}^{3}\overline{A_{ex(i)}}$. Thus the outside spin effectively splits the rotating methyl group center line into two lines, and the value of this splitting, for cases of physical interest, is

(31) P. Devaux and H. M. McConnell, *J. Amer. Chem. Soc.*, 94, 4475 (1972).
(32) E. R. Andrew and R. Bersohn, *J. Chem. Phys.*, 18, 159 (1950).
(33) T. B. Cobb and C. S. Johnson, Jr., *J. Chem. Phys.*, 52, 6224 (1970).

Table II. Spin Functions for the Special Four-Spin Group[a]

$\psi_1 = \alpha_{ex}\alpha\alpha\alpha$	$\psi_7 = \beta_{ex}(\beta\beta\alpha + \beta\alpha\beta + \alpha\beta\beta)(1/\sqrt{3})$
$\psi_2 = \alpha_{ex}(\alpha\alpha\beta + \alpha\beta\alpha + \beta\alpha\alpha)(1/\sqrt{3})$	$\psi_8 = \beta_{ex}(\beta\beta\beta)$
$\psi_3 = \beta_{ex}(\alpha\alpha\alpha)$	$\psi_9 = \alpha_{ex}(\alpha\alpha\beta - \alpha\beta\alpha)(1/\sqrt{2})$
$\psi_4 = \alpha_{ex}(\alpha\beta\beta + \beta\alpha\beta + \beta\beta\alpha)(1/\sqrt{3})$	$\psi_{10} = \alpha_{ex}(\beta\beta\alpha - \beta\alpha\beta)(1/\sqrt{2})$
$\psi_5 = \beta_{ex}(\alpha\alpha\beta + \alpha\beta\alpha + \beta\alpha\alpha)(1/\sqrt{3})$	$\psi_{11} = \beta_{ex}(\alpha\alpha\beta - \alpha\beta\alpha)(1/\sqrt{2})$
$\psi_6 = \alpha_{ex}(\beta\beta\beta)$	$\psi_{12} = \beta_{ex}(\beta\beta\alpha - \beta\alpha\beta)(1/\sqrt{2})$

[a] The subscript ex denotes the outside spin, mentioned in the text, which is distinguishable from the three spins of the methyl top.

both small and dependent on the parameter θ_m'. The motional averaging produced in the broad part of the spectrum by fluctuations in θ_m' is accompanied by averaging of this narrow part for the same reasons. The approximation made in regarding the outside spin as producing a simple fluctuating dipolar field is therefore justified, and the "scaling in" of the spectrum in the presence of motion which results from these conditions is clearly seen in Figure 6.

The dashed line in this figure is the calculated pmr spectrum for methyl groups experiencing rapid rotation about their C_3 axes and undergoing restricted motions in this axis, of amplitude $\Delta\theta_m' = 10°$. These methyl groups also experience a dipolar field from "outside" protons of ~0.5 G, a value typical for the field of neighbor methylene protons at the average position of the methyl protons. The solid line in the figure depicts the spectrum of these methyl groups under the same conditions of internal rotation and neighbor proton fields, but now the amplitude of restricted motion of the C_3 axes is $\Delta\theta_m' = 70°$. As can be seen, the center peak of the spectrum has a width of a few hundred hertz, comparable with the experimental line widths of 150–200 Hz observed for both choline and chain terminal methyl protons in lecithin bilayers.[23] The short vertical bars next to this peak in the figure represent the approximate width of the delayed Fourier transform (FT) "window," that is, the part of the spectrum (in this case the methyl center peaks) which is not filtered out by the acquisition delay in the delayed Fourier transform experiments.[23] Thus most of the methyl center peak from a methyl group undergoing restricted motions of amplitude $\Delta\theta_m' = 70°$ should appear in a delayed FT spectrum, with a width of ~200 Hz, and this calculation agrees well with the observed data.

This situation is not unusual and has been observed in several different types of magnetic resonance spectroscopy as well. Hubbell and McConnell[34] have analyzed partially averaged hyperfine splittings in esr spectra of spin labels incorporated into bilayer systems. These effects arise because a term in the esr spin Hamiltonian, which is the analog of the dipolar term above, cannot be completely averaged by the motions of the spin label. Shporer and Civan[35,36] have also reported nuclear quadrupole resonance (nqr) spectra, from ^{23}Na in sodium linoleate bilayers and $H_2{}^{17}O$ in frog muscle,

(34) W. L. Hubbell and H. M. McConnell, *J. Amer. Chem. Soc.*, 93, 314 (1971).
(35) M. Shporer and M. Civan, *Biophys. J.*, 12, 114 (1972).
(36) M. Civan and M. Shporer, *Biophys. J.*, 12, 404 (1972).

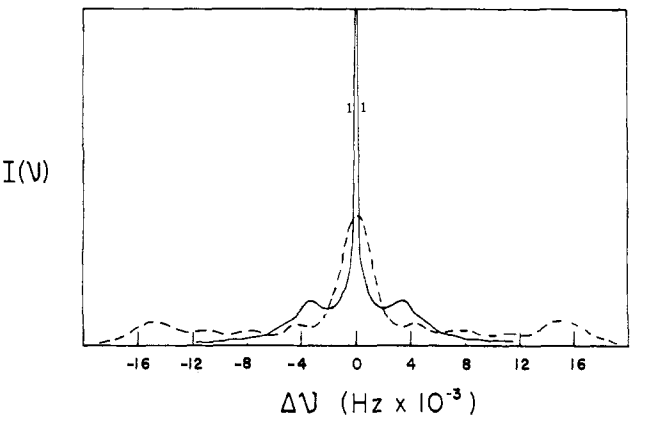

Figure 6. Pmr spectra of "methyl rotors." The dashed line is the spectrum of rapidly reorienting methyl tops whose C_3 axes are allowed to perform restricted motions of amplitude $\Delta\theta_m' = 10°$. The spectrum includes the effects of neighbor protons to the three-spin group. The solid line is the spectrum of the same methyls, except that $\Delta\theta_m'$ is now taken as 70°. The vertical bars next to the resultant motionally narrowed methyl center spike represent the effective width of the delayed Fourier transform "window," that is, the maximum width of the resonance lines which can be observed in a typical delayed FT experiment.

which show partially averaged quadrupole splittings. The situation in these nqr spectra is analogous to that in the methyl group pmr spectra considered here. In both cases, an apparent intensity anomaly arises because solid-like splittings, too large to be observed except on wide-line spectrometers, leave a central peak of much less than 100% intensity.

Discussion

Implication for Bilayers. A motional model of lipid bilayers, which takes into account both chain motions and the motion of polar head groups (*e.g.*, choline in the case of lecithin), can now be brought forth from these calculated spectra. This presentation must start with a review of the experimental pmr line width information which the model must be able to explain. Such information is of two distinct types, that referring to chain protons and that referring to the special case of methyl protons.

The protons of lipid chains in bilayers have a pmr line width, in the usual case, of 3000 Hz, the range of possible line widths covering 2500 to 5000 Hz. The line width can be shown[13,16] to be independent of the applied magnetic field. Furthermore, the line width of an oriented bilayer sample depends on the angle of the lipid chains to the applied magnetic field.[17,20]

The protons of chain terminal methyl groups in bilayers, and the protons of the choline head group in lecithin bilayers, show pmr spectra in which peaks of width ~100–200 Hz are found to contain much less than 100% of the signal intensity expected from the concentration of the protons in the sample. The usual intensity for both types of methyl proton is near 50%, but the intensity of the chain terminal proton signal can be made to increase somewhat with temperature.[23]

One immediate conclusion from these data is that the motion of methyl groups on the choline moiety of lecithin in bilayers is seriously restricted and that a spectrum of the type shown in Figure 6 is observed from these choline methyl protons. This conclusion is quite straightforward, as it is generally believed that

the surface of the bilayer is rigid because of strong charged-group interactions.

A more important conclusion, however, is that the interior of the bilayer has a significant degree of order. A model of motion in which chain protons undergo rapid motion around the chain axis while performing restricted off-axis flexing motions ($\Delta\beta \sim 60°$) accounts for the observed pmr line width of unsonicated bilayers and the variation of this line width in sample orientation experiments. This motional model, here described chiefly in terms of degree of motional restriction, may be compared with conventional physical models of chain motion, and it is possible to decide which of these models, *e.g.*, trans–gauche rotations,[37] gauche$^+$–gauche$^-$ rotation pairs,[37,38] or kink formation,[39] this current picture most closely resembles.

Trans–gauche rotations occur about a single bond and bend the hydrocarbon chain at the point of rotation. Thus, although this mode provides the desired motion for a given proton pair, it would not maintain a sufficient degree of motional restriction for chain terminal methyl groups, as numerous bends in the chain would allow segments near the end to take an almost random orientation. Trans–gauche rotations are therefore not a good description of the flexing of chains in unsonicated bilayers.

Gauche$^+$–gauche$^-$ rotations or kink formation, which are essentially equivalent operations on a hydrocarbon chain, allow suitable motion for individual proton pairs and also maintain segment-wise chain orientation. Because this mode of motion does not swing chain sections out of their orientation perpendicular to the bilayer surface, it permits the chains to stay in a relatively solid-like packing. This feature, the maintenance of packing order, is important because it implies that the motion even of the chain terminal methyl groups will be restricted, and thus the characteristic restricted motion spectrum of methyl groups (Figure 6) would explain the signal intensity anomaly and the narrow line width observed in the pmr spectra of these protons. The amplitude of flexing associated with this motion is of the order $\Delta\beta \sim 60°$, as required from line width considerations. Furthermore, kink formation on a part of the chain near the ionic head causes rotation of the rest of the chain with no associated local flexing, thus producing the condition $\tau_\parallel < \tau_\perp$ for the chain methylene protons. In summary, the motion of chains in unsonicated bilayers resembles sterically the motion of chains in solid polyethylenes[40] or paraffins but occurs on a faster time scale.

T_1 Interpretation. The motional model derived above from line width considerations should also agree with the observed results on spin–lattice relaxation. The most important of these results is the observation that, over a wide range of temperatures and frequencies, the bulk proton spin magnetization recovery in a lipid bilayer proceeds with a single spin–lattice relaxation rate. This result has two main implications. First, the dipole–dipole coupling of the methylene spins must be sufficiently strong that spin diffusion[41] must be invoked to explain why these methylene protons do not exhibit different T_1's. Spin diffusion to those spins with efficient thermal relaxation is characteristic of samples with broad resonance line widths and has been demonstrated to control T_1 in solid and semisolid hydrocarbons.[38] Second, the methyl protons in the bilayer account for 20% of all the protons in the sample and could introduce nonexponentiality into the bulk magnetization recovery if their T_1 were very different from that of the methylene system. Experimentally, the methyl proton magnetization recovery has been observed[23] separately from the bulk and is found to be exponential, with a T_1 close to but not identical with that of the methylenes.

Analysis of the proton T_1 data from unsonicated lipid bilayers could then be expected to yield motional information about two species of protons: those protons which act as the "heat sink" for the spin diffusion process and hence determine the T_1 of the methylene system; and the methyl protons, which relax independently of the methylenes. The T_1 process is more sensitive to motions which are more rapid and of smaller amplitude than those motions which determine the restricted-motion line width, and the T_1 analysis should supplement and independently confirm the motional results of line width analysis.

Motional information about these protons can be obtained from T_1 data using a modification of a formula of Woessner[42] for relaxation by anisotropic motion. This formula is applicable to relaxation of pairs of methylene protons and is extended to relaxation of methyl groups by assuming an uncorrelated contribution to relaxation from the additional proton.[42,43] The same result has been obtained in a much more general form by McBrierty and Douglass,[44,45] but the following specialization is adequate for the bilayer problem and allows a quantitative discussion of local motions. The evaluation only of the intramolecular contribution to T_1 in this case can be justified by reference to experimentally measured intermolecular T_1 contributions.[10]

The well-known formula

$$\frac{1}{T_1} = \frac{9}{8}\frac{\gamma^4\hbar^2}{r^6}\{J_1(\omega_0) + J_2(2\omega_0)\} \tag{16}$$

where

$$J_k(\omega) = \int_{-\infty}^{+\infty} e^{i\omega\tau}\overline{F_k(\tau)F_k(0)}\mathrm{d}\tau \tag{17}$$

$$F_1(\tau) = \sin\theta(\tau)\cos\theta(\tau) \tag{18}$$

and

$$F_2(\tau) = \sin^2\theta(\tau) \tag{19}$$

can be expanded explicitly for a model of anisotropic motion of a pair of spins such as that illustrated in Figure 2. That is, motion of the axis **c** occurs on a time scale $\tau_\perp$, and motion of the pair about this **c** axis occurs on a time scale $\tau_\parallel$. In Woessner's formulation β is fixed (here $\beta = 90°$) and θ' is allowed to fluctuate.

(37) P. J. Flory, "Statistical Mechanics of Chain Molecules," Interscience, New York, N. Y., 1969, p 60.
(38) K. van Putte, *J. Magn. Resonance*, **2**, 216 (1970).
(39) H. Traüble, *J. Membrane Biol.*, **4**, 193 (1971).
(40) N. Pechhold, S. Blasenbrey, and S. Woerner, *Z. Kolloid.*, **189**, 14 (1963).
(41) A. Abragam, "The Principles of Nuclear Magnetism," Oxford University Press, London, Chapter 5, 1961.
(42) D. E. Woessner, *J. Chem. Phys.*, **36**, 1 (1962).
(43) P. S. Hubbard, *Phys. Rev.*, **109**, 1153 (1958).
(44) V. J. McBrierty and D. C. Douglass, *J. Magn. Resonance*, **2**, 353 (1970).
(45) V. J. McBrierty, D. W. McCall, D. C. Douglass, and D. R. Falcone, *J. Chem. Phys.*, **52**, 512 (1970).

Motion about the c axis occurs on a time scale $\tau_{\parallel}$, and motion in θ' occurs on a time scale $\tau_{\perp}$. Because $\beta = 90°$ and free motion around c is allowed, the averaging range $\Delta\theta'$ based on Woessner's treatment is exactly equivalent to the range $\Delta\beta$ used in our line width calculations. Defining a new correlation time τ_c as

$$\frac{1}{\tau_c} = \frac{1}{\tau_{\perp}} + \frac{1}{\tau_{\parallel}}$$

eq 16 becomes

$$\frac{1}{T_1} = \frac{9}{8}\frac{\gamma^4\hbar^2}{r^6}\left\{\frac{1}{4}\overline{(\sin\theta'\cos\theta')^2}\frac{2\tau_{\perp}}{1+\omega_0^2\tau_{\perp}^2} + \frac{1}{8}\overline{\sin^2\theta'(1+\cos^2\theta')}\frac{2\tau_c}{1+\omega_0^2\tau_c^2} + \frac{1}{4}\overline{(\sin^2\theta')^2}\frac{2\tau_{\perp}}{1+4\omega_0^2\tau_{\perp}^2} + \frac{1}{8}\overline{(1+6\cos^2\theta'+\cos^4\theta')}\frac{2\tau_c}{1+4\omega_0^2\tau_c^2}\right\} \quad (20)$$

where the bars denote averaging over the appropriate angular ranges indicated by the restricted motions. This same equation may also be used to calculate the T_1 of methyl protons, using the assumption of independent relaxation contributions among the three protons. The only modifications are that θ' is replaced by θ_m' and the motion characterized by $\tau_{\parallel}$ takes place about the methyl C_3 axis. The distinctive feature of eq 20 is the complex frequency and temperature dependence of T_1 brought about by the introduction of two correlation times. A plot of T_1 *vs.* temperature will usually have a special "double-minimum" form, since activation energies for the processes producing the two motions will not in general be equal. Likewise, a plot of T_1 *vs.* frequency at a given temperature will show a broader T_1 minimum region than will a plot based on a single correlation time model. These two types of plot will contain sufficient information to determine both $\tau_{\perp}$ and $\tau_{\parallel}$. Physically, this result comes about because the type of local field fluctuations which are most efficient for spin–lattice relaxation, *i.e.*, those on the time scale $1/\omega_0$, may occur in two different ways in this model, and variations of temperature or resonance frequency can determine which mode of motion is more efficient for relaxation under different conditions.

T_1 data from egg lecithin and dimyristoyl lecithin bilayers can be analyzed with eq 20 to yield information about $\Delta\theta'$ ($=\Delta\beta$), $\tau_{\perp}$, and $\tau_{\parallel}$ for those protons for which sufficient data are available. The details of the calculation[46] will be reported in detail elsewhere. For the purposes of this paper it is only necessary to summarize the results. First, the condition $\Delta\beta \geq 60°$ is needed to provide an exponential decay, for both the methyl and methylene protons. Second, those protons which act as the heat sink for the methylene system (perhaps those protons near the end of the chains) have the motional time scale $\tau_{\perp} \sim 10^{-7}$ sec and $\tau_{\parallel} \sim 10^{-9}$ sec. The methyl protons are found to have essentially the same $\tau_{\perp}$ but a faster $\tau_{\parallel}$, on the order of 10^{-10} sec.

The relation of these correlation times to the line width results is physically different from their relation to spin–lattice relaxation and should be clarified. First as long as $\tau_{\perp} < 1/\alpha$, there will be significant motional narrowing of the rigid lattice spectrum, but after this condition is fulfilled the line width for restricted motion will depend on $\Delta\beta$ more directly than on $\tau_{\perp}$. Second, the condition $\tau_{\perp} \gg \tau$ reduces the line width (for restricted motions again) by a factor of 2 from what it would be with $\tau_{\perp} \leq \tau_{\parallel}$, and the exact value of $\tau_{\parallel}$ has no further effect on line width even though it is quite important in T_1 considerations. Third, the relationship of these correlation times to line width is quite different in sonicated *vs.* unsonicated bilayers, but we postpone discussion of this topic to a later section below.

T_2 Interpretation in the Limit of Rapid Spin Diffusion. A treatment of T_2 interpretation for methyl spectra analogous to the T_1 theory was presented earlier by the authors[47] and can be seen in the light of present results to apply only to certain special cases. When there are rapid ($\sim$2000/sec) $\alpha \rightarrow \beta$ spin flips among the chain methylene protons (*i.e.*, a case of fast spin diffusion), the terminal methyl protons experience a rapidly alternating dipolar field produced by their neighbor methylene protons. This field is then averaged to zero on a time scale which is fast compared with the inverse of the splitting (called $^4/_3x''$ in the exact treatment above) it induced in the static case in the center peak of the methyl spectrum. Under these conditions it is appropriate to describe the relaxation of this center peak using a pseudo-Hamiltonian in which $\overline{\mathcal{H}_1(t)} = 0$. Then only fluctuations in local fields, and not average values of these fields, contribute to the line width, and the equation

$$\frac{1}{T_2} = \frac{9}{8}\frac{\gamma^4\hbar^2}{r^6}\left\{\frac{1}{4}J_0(0) + \frac{5}{2}J_1(\omega_0) + \frac{1}{4}J_2(2\omega_0)\right\} \quad (21)$$

(where $J_0(0)$ is specified by eq 17 and the definition $F_0(\tau) = 3\cos^2\theta(\tau - 1)$) can be developed for restricted motions by averaging the angular functions involved in the spectral density functions J_k over the appropriate restricted angular ranges. The results reported in ref 47 follow from this simple procedure, except that the calculated intensities reported there are twice as large as they should be because they concern only the center peak and not the whole methyl spectrum.

This physical situation would conceivably occur in samples of mixed phospholipid–cholesterol bilayers. There the cholesterol packing produces considerable additional motional restriction on the methylene chains, while leaving terminal methyls more freedom than in pure lipid bilayers.

Formal Treatment of the Narrowing Effects of Restricted Motions. The chief features of motional narrowing by restricted motions may be explained in terms of the density matrix formalism for relaxation.[48] The time-dependent behavior of the density matrix is expressed by the equation

$$d\rho/dt = \overline{-i[\mathcal{H}_0 + \mathcal{H}_1(t),\rho]} \quad (22)$$

where ρ is the density matrix, $\mathcal{H}_0$ represents the static magnetic Hamiltonian in units of $\hbar$, arising from the applied magnetic field $\mathbf{H}_0$, and $\mathcal{H}_1(t)$ denotes the fluctuating intramolecular dipolar field energy modulated by the motions of the spins. The term $\mathcal{H}_1(t)$ can be made to

(46) G. W. Feigenson and S. I. Chan, submitted for publication.

(47) S. I. Chan, C. H. A. Seiter, and G. W. Feigenson, *Biochem. Biophys. Res. Commun.*, **46**, 1488 (1972).

(48) See ref 41, p 276.

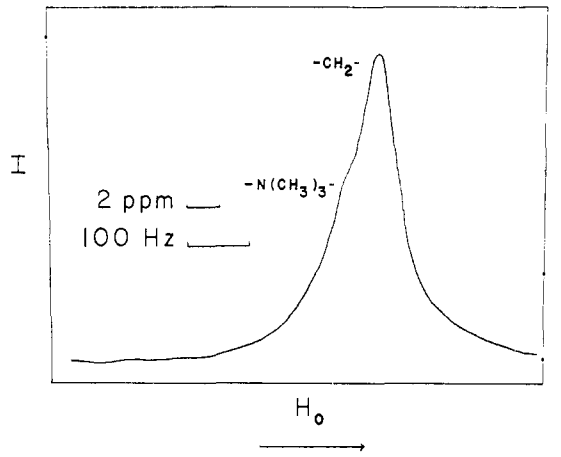

Figure 7. Waugh multipulse-narrowed lecithin pmr spectrum. This spectrum at 55 MHz of dimyristoyl lecithin bilayers was narrowed from an original width of ~3000 Hz by a Waugh multipulse sequence, with 60 μsec cycle time for a complete eight-pulse cycle and instrumental resolution ~10 Hz. The chemical shift reference has been corrected for the scaling effect of the pulse sequence. The choline methyl and chain methylene protons (2.1-ppm separation) can be distinguished.

include other forms of magnetic energy, *e.g.*, anisotropic chemical shift interactions or intermolecular dipolar interactions, when these are felt to be important.

The process of deriving useful relaxation expressions from this equation starts with a transformation of ρ and $\mathcal{H}_1(t)$ to the interaction representation to remove the trivial time dependence of ρ on $\mathcal{H}_0$. This transformation, namely

$$\rho^* = \exp(i\mathcal{H}_0 t)\rho \exp(-i\mathcal{H}_0 t) \tag{23}$$

and

$$\mathcal{H}_1^*(t) = \exp(i\mathcal{H}_0 t)\mathcal{H}_1(t) \exp(-i\mathcal{H}_0) \tag{24}$$

introduces new variables ρ^* and $\mathcal{H}_1^*$, which may simply be thought of as ρ and $\mathcal{H}_1$ viewed in a "rotating frame" rotating at a frequency $\omega_0 = \mathcal{H}_0/\hbar$. The time-dependent behavior of the density matrix reduces after this transformation to

$$d\rho^*/dt = -i\overline{[\mathcal{H}_1^*(t),\rho^*]} \tag{25}$$

which can then be integrated by successive approximation to yield a series expansion for $\rho^*(t)$. An expression for the time derivative of $\rho^*(t)$, accurate to second order, may be obtained by substituting the first-order solution for $\rho^*(t)$ into eq 25. The result is

$$d\rho^*/dt = -i\overline{[\mathcal{H}_1^*(t),\rho^*(0)]} - \int_0^t \overline{[\mathcal{H}_1^*(t),[\mathcal{H}_1^*(t'),\rho^*(0)]]}dt' \tag{26}$$

If $\overline{\mathcal{H}_1}$, and hence $\overline{\mathcal{H}_1^*}$, happens to be zero, this equation simplifies to

$$d\rho^*/dt = -\int_0^t \overline{[\mathcal{H}_1^*(t),[\mathcal{H}_1^*(t'),\rho^*(0)]]}dt' \tag{27}$$

an expression which describes the relaxation of ρ^* in terms of the fluctuations in $\mathcal{H}_1^*(t)$. This result reduces in most cases to familiar expressions for T_1 and T_2, since the terms under the averaging bar are just correlation functions for the appropriate fluctuating fields.

The treatment above, in which $\overline{\mathcal{H}_1} = 0$, applies to the situation of motional narrowing in liquids. However, in the case of restricted motion, the local fluctuating fields do not average to zero, that is $\overline{\mathcal{H}_1} \neq 0$, and the derivation must be modified. This is done most conveniently by separating $\mathcal{H}_1(t)$ into a constant-average part and a time-dependent part, as

$$\mathcal{H}_1(t) = \overline{\mathcal{H}_1} + \mathcal{H}_1'(t) \tag{28}$$

and combining $\overline{\mathcal{H}_1}$ with the static Zeeman Hamiltonian $\mathcal{H}_0$. The master equation, rewritten in terms of this redefined $\mathcal{H}_1(t)$, is

$$d\rho/dt = -i[(\mathcal{H}_0 + \overline{\mathcal{H}_1}) + \mathcal{H}_1'(t),\rho] \tag{29}$$

which can be converted into an expression analogous to eq 27 after ρ and $\mathcal{H}_1'(t)$ are transformed into the interaction representation based on the new static Hamiltonian, *i.e.*

$$\rho^* = \exp[i(\mathcal{H}_0 + \overline{\mathcal{H}_1})t]\rho \exp[-i(\mathcal{H}_0 + \overline{\mathcal{H}_1})t] \tag{30}$$

and

$$\mathcal{H}_1'^*(t) = \exp[i(\mathcal{H}_0 + \overline{\mathcal{H}_1})t]\mathcal{H}_1'(t) \exp[-i(\mathcal{H}_0 + \overline{\mathcal{H}_1})t] \tag{31}$$

Since different spins in the sample experience different values of $\overline{\mathcal{H}_1}$, the calculation must use a distribution of rotating frames corresponding to these different values of $\overline{\mathcal{H}_1}$. Whereas the usual relaxation problem is to find the width of a single resonance signal centered at frequency $\omega_0 = \mathcal{H}_0/\hbar$, this problem involves finding the widths of each resonance line over a distribution of frequencies $\omega' = (\mathcal{H}_0 + \overline{\mathcal{H}_1})/\hbar$. The resonance line shape which is calculated in this way is thus the envelope of a distribution of broadened resonance spikes.

The width of these individual resonance spikes may be investigated by means of the Waugh multipulse averaging sequence.[49,50] This sequence essentially averages $\mathcal{H}_1$ to zero at a rate which is fast compared with the effective dipolar interaction. If, however, local motions are fast compared with the time scale of the pulse cycle, the resulting line width observed in the spectrum measures these local field fluctuations, which are not affected by this sequence.

A spectrum obtained[51] by performing this averaging sequence on a sample of unsonicated dimyristoyl lecithin bilayers is shown in Figure 7. The pulse cycle time was 60 μsec for an eight-pulse sequence and the instrumental resolution was ~10 Hz. Since the intermolecular dipolar broadening can be estimated as ~20 Hz or less[30] in this case, the observed methylene proton line width of ~100 Hz measures essentially the residual intramolecular dipolar broadening. The correlation times corresponding to this width are $\tau_\perp \sim 10^{-7}$ sec and $\tau_\uparrow$ any time shorter than this $\tau_\perp$. This method provides an independent test of the $\tau_\perp$ obtained from T_1 studies and confirms the physical picture of the local motions of chains in unsonicated bilayers.

(49) U. Haeberlen and J. S. Waugh, *Phys. Rev.*, 175, 453 (1968).
(50) U. Haeberlen and J. S. Waugh, *Phys. Rev.*, 185, 420 (1969).
(51) R. W. Vaughan, C. H. A. Seiter, G. W. Feigenson, and S. I. Chan, submitted for publication.

Effect of Sonication. When bilayer sheets are subjected to prolonged ultrasonication they break up, forming in water a dispersion of small vesicles (~300-Å diameter).[52] These vesicles tumble freely and therefore present a different motional narrowing problem from that encountered with bilayer sheets. Specifically, sonicated preparations of lipids show pmr signals which are only a few hertz in width. Furthermore, these signals show essentially 100% of the intensities expected, for all protons of the lipids.[53] Attempts have been made to account for this drastic narrowing of the resonance lines in terms of the effect of overall tumbling of the vesicles.[54] Other explanations hold that increased local motion due to irregularity of chain packing in the small vesicles produces the narrow lines.[55]

This question can be decided using Anderson theory and involves only formulating a motional model for chain protons in these vesicles, deriving a form for $\omega(\tau)$, and evaluating T_2 by the method suggested in eq 5. The calculation will be performed for a pair of neighbor protons on a chain, since this will furnish a minimum intramolecular dipolar line width, and thus provide a lower limit to the degree of local motion present in sonicated vesicles.

The protons on lipid chains in sonicated bilayer vesicles have a complex overall motion which can be described with reference to Figure 2. Let **r** in this figure be an interpair vector and **c** be the lipid chain axis vector. Then the motion has three parts: (i) motion of **c**, because of overall vesicle tumbling, on a time scale τ_v, (ii) motion of **r** with respect to **c**, causing changes in the angle β of **r** to **c**, on a time scale $\tau_\perp$, and (iii) motion of **r** around **c**, causing changes in the angle φ, on a time scale $\tau_\parallel$. The angular part of the dipole–dipole interaction, in terms of the angles described in Figure 2, may then be written as

$$3\cos^2\theta - 1 = \frac{1}{2}(3\cos^2\theta' - 1)(3\cos^2\beta - 1) + 3\sin\theta'\cos\theta'\sin\beta\cos\beta\cos\varphi + {}^3/_2\sin^2\theta'\sin^2\beta\cos 2\varphi \quad (32)$$

Now the line width problem will reduce to calculating the average time fluctuations of this $(3\cos^2\theta - 1)$, given a model of vesicle tumbling for fluctuations in θ' and a model of local motion for fluctuations in β and φ.

It will be helpful to demonstrate an exact T_2 calculation for the case in which only one random function of time need be considered, instead of several as is the case in eq 32. For isotropic motion of a pair of spins, the free induction decay $g(t)$ may be written as

$$g(t) = \overline{\cos\left[\int_0^t \alpha(3\cos^2\theta(\tau) - 1)\mathrm{d}\tau\right]} = \overline{\cos\left[\alpha\int_0^t \sqrt{4/5}\,p(\tau)\mathrm{d}\tau\right]} \quad (33)$$

where $p(\tau)$ is a random function such that $\bar{p} = 0$ and $\overline{p^2} = 1$. For times long compared with the time scale τ_c of the isotropic motion, the integral in eq 33 becomes

$$\alpha\int_0^t \sqrt{4/5}\,p(\tau)\mathrm{d}\tau = \alpha\sqrt{4/5}\,\sqrt{t\tau_c} \quad (34)$$

The value

$$1/T_2 = {}^4/_5\alpha^2\tau_c$$

is then obtained by setting the right-hand side of eq 34 equal to 1, the procedure mentioned earlier (eq 5). This T_2 is identical with that of Kubo and Tomita[24] for the conditions of interest here ($T_1 \gg T_2$).

This procedure is the basis of the T_2 calculation and is modified only by the need for dealing with the several random functions $\theta'(\tau)$, $\beta(\tau)$, and $\varphi(\tau)$ on the right-hand side of eq 32. Evaluation of $\int_0^t(3\cos^2\theta(\tau) - 1)\mathrm{d}\tau$, as given in eq 32, requires two results on random functions. First, any random function $a(t)$ may be represented in the form

$$a(t) = \bar{a} + \{\overline{[a(t) - \bar{a}]^2}\}^{1/2}p(t) \quad (35)$$

where $\overline{(a(t) - \bar{a})^2}$ is now just a constant (*i.e.*, some average value, as denoted by the bar) and p is a new function of the type used in eq 33, such that $\bar{p} = 0$ and $\overline{p^2} = 1$. Second, the product of two random functions p_1 and p_2 of this type is a new function q, where $\bar{q} = 0$ and $\overline{q^2} = 1$, that has an effective correlation time τ_q such that

$$\frac{1}{\tau_q} = \frac{1}{\tau_{p_1}} + \frac{1}{\tau_{p_2}} \quad (36)$$

This expression is correct when p_1 and p_2 are uncorrelated, as will be the case for vesicle tumbling and local motion. An immediate consequence of this result is that the effective correlation times of the second and third terms on the right-hand side of eq 32 are of the order of $\tau_\parallel$, which is the fastest correlation time in the model. These terms can be neglected in comparison with the first, as their inclusion would lead only to a slightly greater line width. With this simplification, and results 35 and 36, the form of $\int_0^t\omega(\tau)\mathrm{d}\tau$ becomes

$$\int_0^t \omega(\tau)\mathrm{d}\tau = \frac{1}{2}\alpha\sqrt{4/5}\{\bar{d}\sqrt{t\tau_v} + (\overline{d'^2})^{1/2}\sqrt{t\tau_*}\} \quad (37)$$

The expression for T_2 is derived as usual by setting eq 37 equal to 1, giving the result

$$1/T_2 = \frac{1}{5}\alpha^2\{\bar{d}^2\tau_v + 2\bar{d}(\overline{d'^2})^{1/2}\sqrt{\tau_v\tau_*} + \overline{d'^2}\tau_*\} \quad (38)$$

where

$$\frac{1}{\tau_*} = \frac{1}{\tau_v} + \frac{1}{\tau_\perp}$$

$$\bar{d} = \overline{(1 - 3\cos^2\beta)}$$

$$\overline{d'^2} = \overline{[\bar{d} - (1 - 3\cos^2\beta)]^2}$$

Since τ_v, $\tau_\perp$, and $\Delta\beta$ are known for a given motional model, this expression gives us a minimum dipolar intramolecular line width under the conditions $\tau_v < 1/(\alpha\bar{d})$ and $\tau_\perp < \tau_v$.

The resulting possible minimum line widths for different motional states are shown in Figure 8. The line width is plotted against values of $\tau_\perp$ for local motion, for different values of $\Delta\beta$ (50, 60, and 70°), and two different vesicle tumbling times (10^{-5} and 10^{-6} sec). These values of $\Delta\beta$ include the range of likely values of this parameter for the local motion in unsonicated bilayers, and the values of τ_v are those possible for small

(52) C. Huang, *Biochemistry*, 8, 344 (1969).
(53) S. A. Penkett, A. G. Flook, and D. Chapman, *Chem. Phys. Lipids*, 2, 273 (1968).
(54) E. G. Finer, A. G. Flook, and H. Hauser, *Biochim. Biophys. Acta*, 260, 49 (1972).
(55) M. P. Sheetz and S. I. Chan, *Biochemistry*, 11, 4573 (1972).

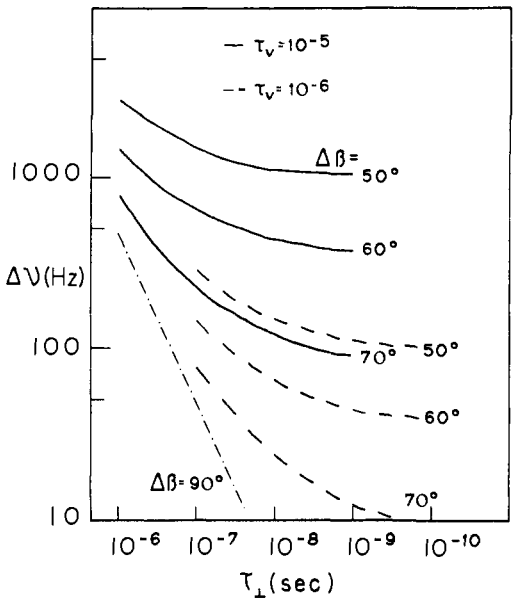

Figure 8. Pmr line width of methylene protons in sonicated bilayers. The line width of a chain methylene proton in a sonicated bilayer vesicle is plotted against $\tau_\perp$, time scale of local flexing motion, for a range of values of $\Delta\beta$ (extent of flexing, as defined in text) and two values of τ_v, vesicle tumbling time. The most probable parameter values are $\tau_v \sim 5 \times 10^{-6}$ sec (250-Å diameter vesicles) and $\Delta\beta \sim 65°$, $\tau_\perp \sim 10^{-7}$ sec (typical local motion in unsonicated bilayers), predicting a line width of several hundred hertz. The dashed and dotted line (–·–) for $\Delta\beta = 90°$ is included for comparison. This line is calculated on the assumption $\tau_\perp < \tau_v$.

(~250-Å diameter) vesicles. The most probable values of all these parameters ($\tau_v \sim 5 \times 10^{-6}$, $\tau_\perp \sim 1 \times 10^{-7}$, $\Delta\beta \sim 60°$) give a line width of several hundred hertz for typical chain protons. Therefore, simple superposition of overall vesicle tumbling on the local motions of chains in bilayers is not enough to explain the line width observed for the chain protons in vesicles. Additional local motion of the lipid chains in vesicles is therefore implied by these line width results. With the help of eq 38, a quantitative estimate of this additional motional freedom may be obtained.

The true pmr line width of methylene protons in vesicles, corrected for chemical shift spread of the methylene region, is approximately 5 Hz.[53] This implies that the sum of the three terms on the right side of eq 38 is 15 sec^{-1} or less. Given $\tau_v \sim 5 \times 10^{-6}$ sec, a representative vesicle tumbling time, this in turn implies values of $\Delta\beta$ greater than 80° and values of $\tau_\perp$ faster than 5×10^{-9}. The amplitudes of local motion are thus significantly larger in sonicated vesicles than in unsonicated bilayers, and the time scale of this motion is roughly 100 times faster.

An immediate consequence of this increased local motion is that the first and second terms on the right in eq 38 become small compared with the third term. Under these conditions the rate of overall vesicle tumbling will not be an important determinant of the line width. Thus changes in solution viscosity, which produce changes in τ_v, should have little effect on observed line widths, and this is found experimentally.[55] As $\Delta\beta \rightarrow 90°$, all motional narrowing is accomplished by the local motion, given $\tau_\perp < \tau_v$, and the effects of tumbling rate are negligible.

Previous treatments of pmr line widths arising from vesicles have met with several difficulties,[54] briefly for lack of a systematic way of dealing with terms other than the first in eq 38. When the local motion is infinitely fast ($\tau_\perp \rightarrow 0$), as these investigators have correctly noted, the line width expression takes the form

$$1/T_2 \sim |\alpha\bar{d}|^2\tau_v \qquad (39)$$

The effective reduced line width $\alpha\bar{d}$ has replaced the usual rigid lattice dipolar width α.[56] In the analogous narrowing problem of "magic angle" sample rotation superimposed on local motion, a similar result is found when the local motion is infinitely fast.

The physical situation, however, for lipid bilayers is that the relevant time scale, $\tau_\perp$, of local motion is not sufficiently fast compared with typical τ_v values that approximation[39] may be used. If a bilayer section could be tumbled at $\tau_v = 5 \times 10^{-6}$ sec with no perturbation of its local structure, the third term in eq 38 would dominate the expression and give a pmr line width for chain protons of several hundred hertz. The effect of a rapid $\tau_\parallel$ has been accounted for by dropping two possible broadening terms in eq 32, and it is important to note the different effects of the $\tau_\perp$ and $\tau_\parallel$ motions, a distinction which is not always appreciated.

Just as the third term in eq 38 represents a broadening contribution which is not removed by vesicle tumbling, a term $1/T\dagger$ appears in the exact treatment of the narrowing effects of the Waugh multipulse sequence,[50] and this broadening contribution is not removed by the pulse sequence. Thus in both coherent (pulse or sample rotation) averaging methods and statistical (Brownian motion) averaging, expressions like eq 39 will generally not be adequate for calculating the line width effects of complicated motions.

The pmr line widths observed from vesicles imply a looser chain packing of the lipids in sonicated bilayers than in unsonicated bilayers. The local motion of chains in vesicles is practically unrestricted and fast ($\tau_\perp < 5 \times 10^{-9}$ sec), and it is the rate of this local motion which controls the line width. This should be contrasted with the situation in unsonicated bilayers, in which chain motion is seriously restricted and slow ($\tau_\perp \sim 10^{-7}$ sec). In terms of the motional model presented earlier, the local motion of chains in vesicles consists of trans–gauche rotations, a mode usually associated with hydrocarbon liquids. This conclusion is compatible with other experimental results on vesicles, most notably measurements of the T_1's of methylene chain ^{13}C nuclei.[57] The lipid chains in sonicated and unsonicated bilayer samples are thus characterized by quite different motional states.

Summary

Two main conclusions about the physical state of the interior of lipid bilayers emerge from these nmr line width results. First, the chief mode of motion of the hydrocarbon chains in unsonicated lipid bilayers is "kink" formation or the related gauche$^+$–gauche$^-$ rotation pair motions. This process occurs at a faster rate in bilayers than in true solids, but as a mode of motion it is nonetheless distinct from the type of chain motions present in hydrocarbon liquids. The lipid

(56) E. R. Andrew and A. Jasinski, *J. Phys. Chem.*, **4**, 391 (1971).
(57) Y. K. Levine, N. J. M. Birdsall, A. G. Lee, and J. C. Metcalfe, *Biochemistry*, 11, 1416 (1972).

chains of sonicated bilayers, on the other hand, have much greater freedom, and the motional state of these chains very nearly resembles a liquid state.

This paper also demonstrates that the stochastic line width theory of Anderson[21] offers the most straightforward way of calculating nmr line widths from spin species undergoing restricted motions and can be readily extended to treat restricted local motions combined with overall Brownian tumbling. Even relatively complex spectra, such as those of methyl groups, may be conveniently simulated for all types of restricted motions. Biological investigations using nmr, for example, studies on tissues, nerves, membranes, or very large molecules frequently demand an understanding of the effects of restricted motion on nmr line widths, and calculations of the type performed here may be necessary.

Acknowledgment. The authors would like to acknowledge many helpful discussions with Mr. G. W. Feigenson and would like to thank Dr. R. W. Vaughan for the use of his multipulse spectrometer.

Assignments in the Natural-Abundance Carbon-13 Nuclear Magnetic Resonance Spectrum of Chlorophyll a and a Study of Segmental Motion in Neat Phytol

Roy A. Goodman, Eric Oldfield, and Adam Allerhand*

Contribution No. 2306 from the Department of Chemistry, Indiana University, Bloomington, Indiana 47401. *Received May 22, 1973*

Abstract: We have recorded the proton-decoupled natural-abundance ^{13}C spectra (at 15.18 MHz) of phytol, phytyl acetate, and chlorophyll a. The 20 carbons of phytol yield 19 peaks. We have assigned 16 out of the 18 single-carbon resonances of phytol to specific carbons with the use of the chemical shift parameters of Grant and Paul, comparisons with the spectrum of pristane and of a phytol–pristane mixture, and ^{13}C spin–lattice relaxation times (T_1) of individual carbons of neat phytol. Even some resonances separated by less than 0.1 ppm arising from structurally very similar carbons near the center of the phytol molecule were specifically assigned. The ^{13}C resonances of phytyl acetate were assigned with the use of single-frequency off-resonance proton decoupling and a comparison with the spectrum of phytol. Phytyl acetate was then used as a model for identifying and assigning all the phytyl carbon resonances in the ^{13}C spectrum of chlorophyll a dissolved in a chloroform–methanol mixture. The T_1 values of neat phytol (at 52°) yielded information about the segmental motions in the branched phytyl chain. The observed behavior is compared with that of the unbranched 1-decanol molecule. While the effective rotational correlation time of the carbons of neat 1-decanol increases monotonically toward the hydroxyl end of the molecule, in the case of phytol there are localized deviations from monotonic behavior, as a result of branching and the presence of an olefinic bond.

Proton nuclear magnetic resonance has been used for investigating the properties of chlorophylls in solution.[1,2] However, even at 220 MHz (51.7 kG), proton nmr spectra of chlorophylls contain very few resolved single-hydrogen resonances, as a result of the small range of proton chemical shifts and the splittings arising from homonuclear scalar coupling. An investigation of the proton-decoupled ^{13}C nmr spectrum of vitamin B_{12} and other corrinoids[3] indicated that ^{13}C nmr is an excellent alternative for studying organic molecules of high complexity. For example, in the proton-decoupled natural-abundance ^{13}C nmr spectrum of cyanocobalamin, more than 40 of the 63 carbons are resolved into single-carbon resonances, even at the relatively low magnetic field of 14.1 kG.[3] Katz and coworkers have reported the ^{13}C nmr spectra of 15% ^{13}C-enriched chlorophyll a and methyl pheophorbide a, recorded at 55 MHz (51.7 kG).[2,4,5] Strouse, Kollman, and Matwiyoff[6] have reported ^{13}C spectra of 90% ^{13}C-enriched chlorophyll a and chlorophyll b at 25.2 MHz (23.5 kG). In the latter work, the use of samples highly enriched in ^{13}C permitted the observation of splittings arising from ^{13}C–^{13}C scalar coupling, which were helpful in assigning the resonances to specific carbons. However, these splittings greatly complicated the spectra and reduced the number of identifiable peaks.

When the percentage of the ^{13}C isotope is small, each carbon yields a single peak (though not necessarily resolved from others) in a proton-decoupled ^{13}C nmr spectrum. There are 55 carbons, all of them nonequivalent, in the chlorophyll a molecule (Figure 1). It seems that when dealing with a system of this complexity, samples of the naturally occurring isotopic composition (1.1% ^{13}C) are most attractive for ^{13}C nmr studies, in terms of spectral simplicity and ease of sample preparation, provided that there is sufficient spectrometer sensitivity for detecting the ^{13}C resonances.

Many resonances in the proton-decoupled ^{13}C nmr spectrum of chlorophyll a have already been assigned to specific carbons.[2,6] However, only carbons 1, 2,

(1) J. J. Katz, R. C. Dougherty, and L. J. Boucher, "The Chlorophylls," L. P. Vernon and G. R. Seely, Ed., Academic Press, New York, N. Y., 1966, Chapter 7.
(2) J. J. Katz and T. R. Janson, *Ann. N. Y. Acad. Sci.*, in press.
(3) D. Doddrell and A. Allerhand, *Proc. Nat. Acad. Sci. U. S.*, 68, 1083 (1971).
(4) J. J. Katz, T. R. Janson, A. G. Kostka, R. A. Uphaus, and G. L. Closs, *J. Amer. Chem. Soc.*, 94, 2883 (1972).
(5) J. J. Katz, *Naturwissenschaften*, 60, 32 (1973).
(6) C. E. Strouse, V. H. Kollman, and N. A. Matwiyoff, *Biochem. Biophys. Res. Commun.*, 46, 328 (1972).